

RESEARCH ARTICLE | FEBRUARY 01 1967

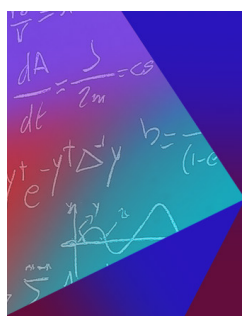
Maximal Analytic Extension of the Kerr Metric

Robert H. Boyer; Richard W. Lindquist



J. Math. Phys. 8, 265–281 (1967)

<https://doi.org/10.1063/1.1705193>



Journal of Mathematical Physics

Young Researcher Award:
Recognizing the Outstanding Work
of Early Career Researchers

[Learn More!](#)



Maximal Analytic Extension of the Kerr Metric*

ROBERT H. BOYER†

Department of Applied Mathematics, University of Liverpool, Liverpool, England

AND

RICHARD W. LINDQUIST

Scott Laboratory of Physics, Wesleyan University, Middletown, Connecticut

(Received 19 July 1966)

Kruskal's transformation of the Schwarzschild metric is generalized to apply to the stationary, axially symmetric vacuum solution of Kerr, and is used to construct a maximal analytic extension of the latter. In the low angular momentum case, $a^2 < m^2$, this extension consists of an infinite sequence Einstein-Rosen bridges joined in time by successive pairs of horizons. The number of distinct asymptotically flat sheets in the extended space can be reduced to four by making suitable identifications. Several properties of the Kerr metric, including the behavior of geodesics lying in the equatorial plane, are examined in some detail. Completeness is demonstrated explicitly for a special class of geodesics, and inferred for all those that do not strike the ring singularity.

I. INTRODUCTION

A FAMILIAR feature of exact solutions to the field equations of general relativity is the presence of singularities. Although long recognized in such special metrics as those of Schwarzschild and Reissner-Nordström, and in the spherically symmetric Friedmann models, these singularities have been dismissed as nonphysical, due perhaps to the high degree of symmetry assumed for the solutions.¹ Recent work by Penrose and Hawking² suggests that this traditional view may need to be revised; it is quite possible that gravitational collapse leads inevitably to a singular state if trapped surfaces are once formed³—provided that one stubbornly persists in applying the classical field equations to regions of arbitrarily high curvature.⁴ Thus there is some point in studying the complete geometry of exact solutions, even though they are idealizations of physically reasonable gravitating systems, in order to learn something about the type of behavior to be

expected in more realistic models. We here lay the foundations for such a study of stationary axially symmetric models of rotating bodies, by analyzing in some detail the empty space metric of Kerr.⁵

Of course one must be careful to distinguish true singularities, to which the Penrose-Hawking theorems refer, from "pseudosingularities" that reflect merely a poor choice of coordinates. The latter can always be removed by the familiar device of covering the manifold with a family of coordinate patches. It has long been recognized that the singularity at $r = 2m$ in the standard form of the Schwarzschild metric is of this type; transformations to coordinate frames which remove this apparent singularity have been given by several authors.⁶

Closely related to the problem of singularities is that of completeness.⁷ Solutions of the field equa-

* R. P. Kerr, *Phys. Rev. Letters* **11**, 237 (1963).

⁵ A. S. Eddington, *Nature* **113**, 192 (1924); this transformation was rediscovered by D. Finkelstein, *Phys. Rev.* **110**, 965 (1958). Other forms of the metric which are nonsingular at the Schwarzschild radius were exhibited by G. Lemaître, *Ann. Soc. Sci. Bruxelles* **53A**, 51 (1933), and by J. L. Synge, *Proc. Roy. Irish Acad.* **A53**, 83 (1950). C. Fronsdal, *Phys. Rev.* **116**, 778 (1959); and J. Plebański, *Bull. Acad. Polon. Sci.* **10**, 373 (1962), independently constructed the maximal analytic extension of the Schwarzschild manifold by imbedding it in a six-dimensional flat space. A transformation to a coordinate frame which displays this maximal extension was first given by M. D. Kruskal, *Phys. Rev.* **119**, 1742 (1960).

⁷ By "completeness" we mean affine completeness: the property that all geodesics can be continued to arbitrarily large values of their affine path parameters. A standard theorem of Riemannian geometry states that geodesic completeness is equivalent to completeness as usually defined—namely, that all Cauchy sequences converge—if the metric is positive definite; however, this theorem breaks down on manifolds with an indefinite metric. For a careful discussion of different possible and inequivalent definitions of completeness for manifolds with an indefinite metric, see W. Kundt, *Z. Physik* **172**, 488 (1963); C. W. Misner, *J. Math. Phys.* **4**, 924 (1963); and M. Fierz and R. Jost, *Helv. Phys. Acta* **38**, 137 (1965).

* Work supported in part by the Aerospace Research Laboratories, Office of Aerospace Research, and by the Office of Scientific Research, U. S. Air Force.

† Deceased.

¹ See, e.g., E. M. Lifshitz and I. M. Khalatnikov, *Zh. Eksperim. i Teor. Fiz.* **39**, 149, 800 (1960) [English transl.: *Soviet Phys.—JETP* **12**, 108, 558 (1961)].

² R. Penrose, *Phys. Rev. Letters* **14**, 57 (1965); S. W. Hawking, *ibid.* **15**, 689 (1965). See also S. W. Hawking and G. F. R. Ellis, *Phys. Letters* **17**, 246 (1965).

³ The collapse of a spherically symmetric mass has been studied in detail by M. M. May and R. H. White, *Phys. Rev.* **141**, 1232 (1966). They find that unless the collapse is halted before any fraction of the total mass has fallen within its own Schwarzschild radius, a singularity invariably ensues.

⁴ Wheeler has repeatedly emphasized that, from a deeper point of view, these singularities must be nonphysical, since quantum effects will necessarily alter the complexion of the problem completely in regions of high curvature. See B. K. Harrison, K. S. Thorne, M. Wakano, and J. A. Wheeler, *Gravitation Theory and Gravitational Collapse* (University of Chicago Press, Chicago, Ill., 1965).

tions are usually presented locally, in terms of a coordinate system adapted to the symmetries of a given problem. Thus the manifold on which the metric is to be defined is left unspecified at the start, and determined only afterwards by imposing various global and topological conditions. Ideally, one would like the resulting manifold to be geodesically complete and free of singularities, but the Penrose-Hawking theorems show that in many cases these two aims are incompatible. Of course, one can always eliminate singularities from a given metric by redefining the manifold to exclude the singular points; this is not a very satisfactory solution, however, if physical test particles run off the edge of the space-time so obtained in a finite proper time. It seems preferable, we believe, to require geodesic completeness, insofar as possible, even though this leads in general to singularities. Thus if \mathfrak{M} and \mathfrak{M}' are analytic manifolds, with $\mathfrak{M}' \supset \mathfrak{M}$, we call \mathfrak{M}' a *maximal analytic extension* of \mathfrak{M} if every geodesic of \mathfrak{M}' is either complete or terminates at a singular point. Such an extension need not exist,⁸ and even if it does it will not be unique, because of the freedom available to identify points in \mathfrak{M}' in a variety of ways without disturbing analyticity.

Analytic Extensions of the Schwarzschild and Reissner-Nordström Metrics

Eddington⁹ long ago pointed out that the transformation

$$r = \bar{r}, \quad \theta = \bar{\theta}, \quad \varphi = \bar{\varphi}, \quad (1.1)$$

$$dt = d\bar{t} + 2m d\bar{r}/(\bar{r} - 2m)$$

(where, to agree with our later notation, we use bars to denote the original coordinates of Schwarzschild) leads to a form of the Schwarzschild metric free of singularities at $\bar{r} = 2m$:

$$ds^2 = dr^2 + r^2(d\theta^2 + \sin^2 \theta d\varphi^2) - dt^2 + (2m/r)(dr + dt)^2. \quad (1.2)$$

This metric, interpreted on the manifold $r > 0$, $0 \leq \theta \leq \pi$, $0 \leq \varphi < 2\pi$, $-\infty < t < \infty$, is in fact an analytic extension of the original; it is complete for $t \rightarrow +\infty$ —excepting those geodesics which strike the true singularity at $r = 0$ —but not for $t \rightarrow -\infty$. One notes that this form has the structure of a flat space metric plus the square of a null vector; this feature serves as the point of departure in the Kerr-Schild⁹ theory, to which we refer briefly in Sec. II. The alternative transformation

$$r' = \bar{r}, \quad \theta' = \bar{\theta}, \quad \varphi' = \bar{\varphi}, \quad (1.3)$$

$$dt' = d\bar{t} - 2m d\bar{r}/(\bar{r} - 2m)$$

leads to an expression for ds^2 similar to (1.2), but with dt replaced by $-dt'$, which is complete for $t' \rightarrow -\infty$. One thus obtains two coordinate patches, shown in Fig. 1, whose domain of overlap is the region external to the Schwarzschild pseudosingularity. This is still not the maximal analytic extension, however. The latter has been given in a particularly simple form by Kruskal,¹⁰ and is summarized by the transformation equations

$$u \pm v = |(r/2m) - 1|^{\frac{1}{2}} \exp [(r \pm t)/4m]. \quad (1.4)$$

The corresponding manifold, illustrated by the now familiar Kruskal diagram (Fig. 1), consists of two asymptotically flat universes whose spacelike sections are joined together on a 2-sphere of minimum area—the “throat” of an Einstein-Rosen bridge.¹⁰ The area of this throat changes with time, reaching a maximum value of $4\pi(2m)^2$ at $u = 0$, $v = 0$, and collapsing to zero both in the future and the past, at those points ($u = 0$, $v = \pm 1$, for instance) for which $r = 0$.

A similar analysis for the Reissner-Nordström solution (the metric outside a single mass m with charge q) has been carried through by Graves and

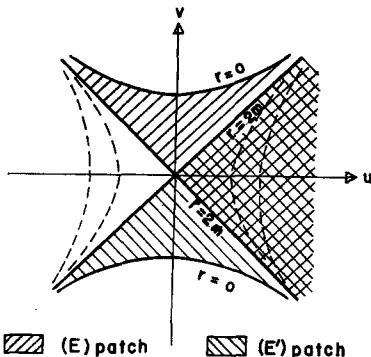


FIG. 1. A Kruskal diagram for the Schwarzschild metric, showing a portion of the (u, v) coordinate plane. In this plane null curves appear as straight lines of slope ± 1 ; the null lines $u \pm v = 0$ define the horizons. The curves $r = \text{const}$ are hyperbolas having these horizons as asymptotes, with the $r = 0$ hyperbola a singular surface. The shaded regions show the portion of the (u, v) plane in which the Eddington coordinates (E) and (E') are regular; their overlap is the region of regularity $u > 0$, $u^2 > v^2$ ($r > 2m$, $-\infty < t < \infty$) for standard Schwarzschild coordinates. The fourth unshaded region, $u < 0$ and $u^2 > v^2$, is also asymptotically flat, and represents the second sheet of an Einstein-Rosen bridge.

⁸ A simple counter-example has been constructed by C. W. Misner, University of Maryland Tech. Rept. No. 529 (1965), p. 14.

⁹ R. P. Kerr and A. Schild, Am. Math. Soc. Symposium, New York, 1964; also Galileo Quatercentenary, Florence, 1964.

¹⁰ A. Einstein and N. Rosen, Phys. Rev. **48**, 73 (1935).

Brill.¹¹ This metric has two pseudosingularities at

$$r = r_{\pm} \equiv m \pm (m^2 - q^2)^{\frac{1}{2}} \quad (1.5)$$

and a true singularity at $r = 0$. Graves and Brill displayed transformations of the Kruskal type which would eliminate either pseudosingularity, but not both. Nevertheless, their results are sufficient to portray the full manifold, for by piecing together successive coordinate patches one can extend the metric first across one singularity and then across the other. It turns out that the resulting manifold is still not complete, however, and one must continue to add similar patches indefinitely. The picture which emerges is thus altogether different from the Schwarzschild case. One can view the manifold as an Einstein-Rosen bridge, whose throat oscillates between a minimum and a maximum area, given by $4\pi r_-^2$ and $4\pi r_+^2$. After each cycle the bridge is found to be attached to a new pair of (asymptotically flat) sheets, isometric to the original pair but nevertheless topologically distinct from them (but see the end of Sec. III).

Horizons

The pseudosingularities $r = r_{\pm}$, like $r = 2m$ in the Schwarzschild metric, have an important geometric and physical significance: They determine the location of horizons. In stationary space-times, these may provisionally¹² be defined as stationary null hypersurfaces: Whenever, for some function $f(r, \theta, \varphi)$, the equation $(\text{grad } f)^2 = 0$ is satisfied on $f = \text{const}$, then this hypersurface is called a horizon. It acts locally as a one-way membrane of infinite red shift (see note added in proof).

Within the horizons of the Schwarzschild and Reissner-Nordström metrics, when such occur, there are trapped surfaces in the sense of Penrose.² Moreover, both metrics contain real singularities, located at $r = 0$ in the coordinates normally used. Time-like paths which cross the horizons of the latter, however, need not strike the singularity, but can be continued onto another sheet and thence out to (another) spatial infinity. The surface $r = 0$ is

simply a barrier that prevents continuation of the metric to negative values of r . As we see presently, on the Kerr manifold $r = 0$ defines a similar barrier, but one of lower dimension, and the extension to negative values of r is meaningful and necessary. Trapped surfaces exist here, too; however, the Penrose-Hawking theorems do not apply to the Reissner-Nordström and Kerr manifolds, for these do not admit the required Cauchy initial hypersurface.

When $q^2 > m^2$, Eq. (1.5) breaks down; there are then no horizons and much of the previous discussion ceases to apply. In fact, the original coordinate patch covers the maximal extension.

Kerr Metric

We have reviewed the above results at length since they bear directly on the problem we wish to consider—that of obtaining a corresponding maximal analytic continuation of the Kerr metric. This solution, it may be recalled, describes a possible exterior field outside a rotating body; it is the only known example of a stationary vacuum metric with gravitational mass and rotation that is asymptotically flat. Like the Schwarzschild metric it is algebraically special (i.e., of type *D* in the Petrov-Pirani classification¹³); thus it contains two geodesic shear-free null congruences.¹⁴ It admits two Killing vectors, associated with time translations and rotations about an axis of symmetry, and it contains two parameters m and a which can be identified with the total mass and angular momentum per unit mass of the source. Although no one has yet succeeded in displaying explicitly an interior metric which fits smoothly onto Kerr's exterior solution, there do not appear to be any difficulties in principle in integrating the combined equations of hydrodynamics and gravitation for the interior case, provided that the shape of the body is chosen appropriately.¹⁵ For purposes of this paper, however, we neglect the presence of any such source, and ask rather for the maximal extension of the empty space metric.

Kerr's solution contains two event horizons, which

¹¹ J. C. Graves and D. R. Brill, *Phys. Rev.* **120**, 1507 (1960). The case $m^2 = q^2$ has been studied by B. Carter, *Phys. Letters* **21**, 423 (1966).

¹² B. Carter (private communication) has stated a theorem which suggests a more stringent definition of a horizon. Briefly: "Let a space-time admit a group of isometries with p -dimensional integral surfaces, and let the tangent p vector be $(4-p)$ -surface orthogonal. Then the locus of nullity of the Killing p vector is itself a null hypersurface." This surface—the "Killing horizon"—appears in the Schwarzschild and Reissner-Nordström metrics with $p = 1$ or 3 and in the Kerr metric (as we see later) with $p = 2$. For a different definition of an "event horizon," see W. Rindler, *Monthly Notices Roy. Astron. Soc.* **116**, 662 (1956).

¹³ A. Z. Petrov, *Sci. Notices, Kazan State Univ.* **114**, 55 (1954); F. A. E. Pirani, *Phys. Rev.* **105**, 1089 (1957).

¹⁴ R. Debever, *Compt. Rend.* **249**, 1324 (1959); R. Penrose, *Ann. Phys. (N. Y.)* **10**, 171 (1960); R. K. Sachs, *Proc. Roy. Soc. (London)* **A264**, 309 (1961).

¹⁵ R. H. Boyer, *Proc. Cambridge Phil. Soc.* **61**, 527 (1965). A. G. Doroshkevich, Ya. B. Zel'dovich and I. D. Novikov, *Zh. Eksperim. i Teor. Fiz.* **49**, 170 (1965) [English transl.: *Soviet Phys.—JETP* **22**, 122 (1966)] claim that the interior solution must also display some type of vortex or convective motion, because the Kerr metric has other off-diagonal components besides $g_{\phi t}$. However, their argument is based upon a false premise; see for example Eq. (2.13).

in an appropriate coordinate system are located at

$$r = r_{\pm} \equiv m \pm (m^2 - a^2)^{1/2} \quad (1.6)$$

plus a true singularity again formally defined by $r = 0$. The correspondence with the Reissner-Nordström result (1.5) is rather striking. Thus one might expect the maximal extension of the Kerr manifold to be topologically very similar to the Graves-Brill construction. A main object of our work is to justify this expectation, by displaying a transformation analogous to that of Kruskal. We give this in detail in Sec. III, after first exhibiting several other useful coordinate frames in Sec. II. Kruskal's method, as generalized by Graves and Brill, cannot be applied directly—except to the two-dimensional subspace containing the symmetry axis and the time coordinate¹⁶—because the metric depends on the polar angle θ in a complicated way. But when we combine a transformation analogous to (1.4) with an appropriate change in the azimuthal angle φ , whose effect is to straighten out the null congruences in the neighborhood of the event horizon being considered, we find, happily, that the resulting metric is regular across the horizon at all values of θ .

The proof that our extension is maximal requires a demonstration that geodesics which do not strike a true singularity can be continued to infinite length. We show this in Sec. IV by studying the geodesic equations. Some particular features of the geodesics themselves, which seemed to us to be interesting and curious, are described briefly in Sec. V.

II. PROPERTIES OF THE KERR METRIC

Kerr-Schild Theory

Kerr and Schild⁹ have studied solutions of the vacuum field equations for which the metric has the form¹⁷

$$g_{\alpha\beta} = \eta_{\alpha\beta} + 2Hk_{\alpha}k_{\beta}. \quad (2.1a)$$

Here $\eta_{\alpha\beta}$ is the metric of Minkowski space, k_{α} a null vector field, H a scalar field. It does not matter whether k_{α} is defined to be null with respect to the flat background metric $\eta_{\alpha\beta}$ or the full metric $g_{\alpha\beta}$, since

$$g^{\alpha\beta}k_{\beta} = \eta^{\alpha\beta}k_{\beta} \equiv k^{\alpha}$$

and therefore $g^{\alpha\beta}k_{\alpha}k_{\beta} = 0$ implies $\eta^{\alpha\beta}k_{\alpha}k_{\beta} = 0$ and conversely. In fact,

$$g^{\alpha\beta} = \eta^{\alpha\beta} - 2Hk^{\alpha}k^{\beta}. \quad (2.1b)$$

¹⁶ B. Carter, Phys. Rev. **141**, 1242 (1966), has independently worked out the analytic extension of this subspace.

¹⁷ Notational conventions: Greek letters range and sum from 1 to 4; $g_{\alpha\beta}$ has signature $(+++-)$.

Kerr and Schild showed that the vacuum field equations require the null congruence to be *geodesic* (with respect to either $g_{\alpha\beta}$ or $\eta_{\alpha\beta}$). By choosing H suitably, k_{α} can be so normalized that

$$k^{\beta}\nabla_{\beta}k^{\alpha} = 0, \quad (2.2a)$$

∇_{β} being the covariant derivative based upon $g_{\alpha\beta}$. We suppose this to be the case, and define an affine parameter μ by $k^{\alpha} = dx^{\alpha}/d\mu$. Then, as Kerr and Schild noted, one finds

$$R_{\alpha\beta\gamma\delta}k^{\beta}k^{\delta} = -(d^2H/d\mu^2)k_{\alpha}k_{\gamma}. \quad (2.2b)$$

It follows that k^{α} is a multiple Debever-Penrose¹⁴ vector, and consequently, by the Goldberg-Sachs¹⁸ theorem, that the null congruence defined by k^{α} is *shear-free* as well.

In their analysis, Kerr and Schild give rules for constructing the general empty-space metric of the form (2.1). We do not quote these here, but merely remark that with the exception of the Kerr metric the representation (2.1) is unique, so that the metric is of type II in the Petrov-Pirani classification.

Kerr Metric in Explicit Form

Let us consider the exceptional case, in which the line element can be represented in the form (2.1) in two distinct ways:

$$g_{\alpha\beta} = \eta_{\alpha\beta} + 2Hk_{\alpha}k_{\beta}, \quad (2.3a)$$

$$\eta'_{\alpha\beta} + 2H'l_{\alpha}l_{\beta}. \quad (2.3b)$$

Both k^{α} and l^{α} are then principal null vectors (i.e., double Debever-Penrose vectors), which implies that the metric is of type *D* (type *I* degenerate). This case is of particular interest, for it describes the stationary vacuum solution with rotation first obtained in a different way by Kerr.⁵ He gives the explicit presentation

$$ds^2 = dx^2 + dy^2 + dz^2 - dt^2 + \frac{2mr^3}{(r^4 + a^2z^2)} \times \left[\frac{r(x dx + y dy) + a(x dy - y dx)}{r^2 + a^2} + \frac{z dz}{r} + dt \right]^2, \quad (2.4)$$

r being defined by

$$[(x^2 + y^2)/(r^2 + a^2)] + z^2/r^2 = 1, \quad (2.5)$$

which corresponds to one of the two forms (2.3). We denote the coordinate system (x, y, z, t) as the (M) frame, and identify it with the form (2.3a) in which

¹⁸ J. N. Goldberg and R. K. Sachs, Acta Phys. Polon. **22**, 13 (1962).

the \mathbf{k} congruence is displayed. The (altogether different) coordinate system (x', y', z', t') adapted to the \mathbf{l} congruence we call the (M') frame. The transformation equations relating these two systems can be worked out from formulas given later in this section.

The form (2.4) of the Kerr metric is inconvenient for many applications, since r is a complicated function of x, y, z . Kerr has given alternative and more suitable form, in which r is one of the coordinates; he applies to Eq. (2.4) the transformation

$$\begin{aligned} x &= (r^2 + a^2)^{1/2} \sin \theta \cos [\varphi - \tan^{-1}(a/r)], \\ y &= (r^2 + a^2)^{1/2} \sin \theta \sin [\varphi - \tan^{-1}(a/r)], \\ z &= r \cos \theta, \end{aligned} \quad (2.6)$$

and obtains

$$\begin{aligned} ds^2 &= dr^2 + 2a \sin^2 \theta dr d\varphi + (r^2 + a^2) \sin^2 \theta d\varphi^2 \\ &+ \Sigma d\theta^2 - dt^2 + (2mr/\Sigma)(dr + a \sin^2 \theta d\varphi + dt)^2. \end{aligned} \quad (2.7)$$

Here

$$\Sigma(r, \theta) \equiv r^2 + a^2 \cos^2 \theta. \quad (2.8)$$

This is a generalization of the Eddington⁶ form of the Schwarzschild metric [cf. Eq. (1.2)]; accordingly, we refer to the coordinate system (r, θ, φ, t) as the (E) frame. Note that in the asymptotic region, $r \rightarrow \infty$, Eq. (2.7) reduces to Eq. (1.2), which justifies the interpretation of the parameter m as the total mass of the source. (We therefore assume $m > 0$.) By comparing higher-order terms with the weak-field metric for a rotating body as given by Landau-Lifshitz,¹⁹ or by calculating the corrections to the perihelion precession formula and comparing with the Lense-Thirring result,²⁰ one can show that the parameter a is just the angular momentum per unit mass of the source. We see later that the Kerr solution radically changes its character for $|a| > m$.

(r, θ, φ) Coordinate Surfaces

To explore the properties of the principal null congruences in greater detail, we find it convenient to study the relation between the (E) and (M) coordinates, by viewing the surfaces $r, \theta, \varphi = \text{const}$ in a Euclidean 3-space whose Cartesian coordinates are (x, y, z) . From Eq. (2.5) it is clear that the surfaces $r = \text{const}$ are confocal ellipsoids, while from

¹⁹ L. D. Landau and E. M. Lifshitz, *Classical Theory of Fields* (Addison-Wesley Publishing Company, Inc., Reading, Mass., 1962), 2nd ed., p. 359.

²⁰ R. H. Boyer and T. G. Price, Proc. Cambridge Phil. Soc. 61, 531 (1965).

$$\frac{x^2 + y^2}{a^2 \sin^2 \theta} - \frac{z^2}{a^2 \cos^2 \theta} = 1 \quad (2.9)$$

it follows that the $\theta = \text{const}$ surfaces are hyperboloids of one sheet, confocal to the ellipsoids. Actually, since z has the same sign as $\cos \theta$, the surface $\theta = \text{const}$ is only a half-hyperboloid, truncated at its waist, lying in the half-space $z \geq 0$ according as $\theta \leq \frac{1}{2}\pi$. Note that at $r = 0$ the ellipsoid degenerates to a disk, $x^2 + y^2 = a^2 \sin^2 \theta$, $z = 0$. The boundary of this disk [where $r = 0$, $\theta = \frac{1}{2}\pi$ and therefore $\Sigma(r, \theta) = 0$] is of particular importance, since it is precisely this set of points at which the metric (2.7) becomes singular.

The surfaces $\varphi = \text{const}$ have the appearance of bent planes, which are approximately vertical for large r but flatten out and become horizontal at the edge of the disk (Fig. 2). Letting φ be fixed but arbitrary, set

$$\xi = x \cos \varphi + y \sin \varphi, \quad \eta = -x \sin \varphi + y \cos \varphi.$$

Equation (2.6) then yields

$$\xi = r \sin \theta, \quad \eta = -a \sin \theta, \quad z = r \cos \theta,$$

or equivalently

$$(a/\eta)^2 - (z/\xi)^2 = 1. \quad (2.10)$$

This defines a ruled quartic surface, whose generators are given by $\eta = -a \sin \theta$, $z = \xi \cot \theta$, with θ held constant on a given generator. (Hence each line is also a generator of the corresponding hyperboloid $\theta = \text{const}$.) Since $\xi = x$, $\eta = y$ for $\varphi = 0$, we have in fact constructed the surface $\varphi = 0$. And because of the way (ξ, η) are related to (x, y) , it is obvious that all the other $\varphi = \text{const}$ surfaces are

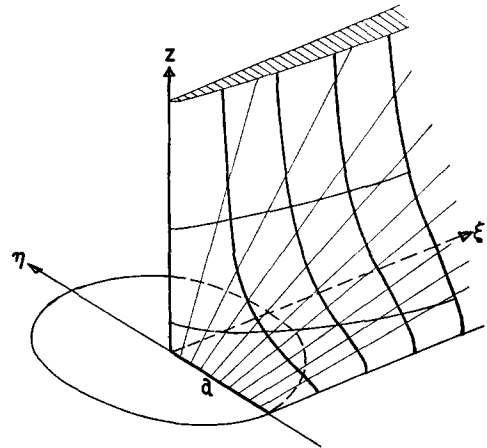


FIG. 2. The ruled quartic surface $\varphi = \text{const}$, shown imbedded in a Euclidean 3-space with Cartesian coordinates (ξ, η, z) .

merely replicas of this one, and can be obtained by rotating it about the z axis.

Throughout the foregoing we have tacitly assumed that r is positive. However, the disk $r = 0$, which has been viewed as a membrane of discontinuity, may just as well be considered a two-sided aperture to a second sheet on which r is negative. Such a continuation to negative r values is permissible because the metric (2.7) remains regular at $r = 0$ (provided $\theta \neq \frac{1}{2}\pi$). We hasten to remark that this second sheet is not to be confused with the other side of an Einstein-Rosen bridge,¹⁰ which one encounters in the familiar Kruskal procedure. We construct an analog of the latter in Sec. III; it has properties quite different from the $r < 0$ extension contemplated here. For one thing, the behavior of the metric as $r \rightarrow -\infty$, with $m > 0$ by definition and therefore m/r negative, describes the sort of geometry one would expect far from a particle of *negative* mass. On the other hand, the two sides of an Einstein-Rosen bridge are isometric, so both describe the field outside a positive-mass body.

In the Kerr-Schild theory the most general metric is determined by an analytic function of one complex variable. For the special case of the Kerr solution, this function has a branch point at the ring singularity $r = 0$, $\theta = \frac{1}{2}\pi$. Thus one can properly view the continuation of (2.7) to negative r values as an analytic continuation onto the second Riemann surface of this function. By passing twice in the same direction through the ring one returns to the original Riemann sheet, and thus to a manifold isometric to the original one, which may for simplicity be identified with it.

"Schwarzschild-Like" Coordinates

Making the transformation

$$\begin{aligned}\bar{r} &= r, & \bar{\theta} &= \theta, \\ d\bar{\varphi} &= d\varphi + a dr/\Delta(r), \\ d\bar{t} &= dt - 2mr dr/\Delta(r),\end{aligned}\quad (2.11)$$

where

$$\Delta(r) \equiv r^2 - 2mr + a^2, \quad (2.12)$$

we find that

$$\begin{aligned}ds^2 &= \Sigma(dr^2/\Delta + d\theta^2) + (r^2 + a^2)\sin^2\theta d\bar{\varphi}^2 - d\bar{t}^2 \\ &\quad + (2mr/\Sigma)(a\sin^2\theta d\bar{\varphi} + d\bar{t})^2.\end{aligned}\quad (2.13)$$

This form has only one off-diagonal component, $g_{\varphi t}$, and is thus invariant under the transformation $\bar{\varphi} \rightarrow -\bar{\varphi}$, $\bar{t} \rightarrow -\bar{t}$. We refer to $(r, \theta, \bar{\varphi}, \bar{t})$ as (S)

coordinates, since they reduce to the standard Schwarzschild coordinates when $a = 0$.

The metric (2.13) has, in addition to the true singularity at $\Sigma = 0$, a pair of pseudosingularities at the real zeros of $\Delta(r)$. The latter are located at

$$r_{\pm} = m \pm (m^2 - a^2)^{\frac{1}{2}} \quad (1.6)$$

and thus exist only when $a^2 \leq m^2$. The close similarity of this equation with the one arising in the Reissner-Nordström problem has already been remarked, as has the identification of the surfaces $r = r_{\pm}$ with stationary null surfaces, or horizons. Let $f = 0$ be any null hypersurface containing the Killing vectors $\partial/\partial\varphi$ and $\partial/\partial t$; then

$$f = f(r, \theta), \quad (\text{grad } f)^2 = 0,$$

and from the contravariant form of the metric [given in Eq. (2.15)] we deduce

$$\Delta(r)(\partial f/\partial r)^2 + (\partial f/\partial \theta)^2 = 0. \quad (2.14)$$

The only solutions of this equation periodic in θ are the ellipsoids $r = r_{\pm}$. The cases $a = m$ and $a = 0$ (Schwarzschild) are seen to be exceptional: In the former case the two horizons coalesce, while in the latter case $r_- = 0$, which is not a null surface at all but an essential singularity.

Because of these additional spurious singularities the (S) coordinates are an inappropriate tool to use in studying the analytic properties of the vacuum metric; evidently in any such investigation the (E) coordinates are far superior.²¹ but the (S) coordinates have one important advantage which we exploit in later sections, namely, they treat both of the principal null congruences on an equal footing.

Principal Null Congruences

The inverse (contravariant) form of Eq. (2.7) is

$$\begin{aligned}(\text{grad})^2 &= \Sigma^{-1} \left[(r^2 + a^2) \left(\frac{\partial}{\partial r} \right)^2 - 2a \left(\frac{\partial}{\partial r} \right) \left(\frac{\partial}{\partial \varphi} \right) \right. \\ &\quad \left. + \frac{1}{\sin^2\theta} \left(\frac{\partial}{\partial \varphi} \right)^2 + \left(\frac{\partial}{\partial \theta} \right)^2 \right] \\ &\quad - \left(\frac{\partial}{\partial t} \right)^2 - \left(\frac{2mr}{\Sigma} \right) \left(\frac{\partial}{\partial r} - \frac{\partial}{\partial t} \right)^2,\end{aligned}\quad (2.15)$$

which is again of the form: flat-space metric plus the square of a null vector [cf. Eq. (2.1b)]. Thus the contravariant components of the null congruence \mathbf{k} can be read off immediately:

$$\mathbf{k} \equiv (k^r, k^\theta, k^\varphi, k^t) = (-1, 0, 0, 1). \quad (2.16a)$$

²¹ This feature of the original Eddington coordinates was first clearly recognized by D. Finkelstein.⁸

With this normalization Eq. (2.2a) is satisfied, and consequently t (or r) is an affine parameter along the congruence. Having chosen $k^t > 0$, we can say that \mathbf{k} is future-pointing, and since $k^r < 0$, we conclude that the \mathbf{k} congruence is *ingoing*.

Next recall that \mathbf{k} must appear as a *linear* congruence when expressed in (M) coordinates. Since $k^\theta = k^\varphi = 0$, such lines must lie in the surfaces $\theta, \varphi = \text{const}$, and are therefore the common generators of these surfaces. As t increases, the rays proceed inwards toward the disk $r = 0$, cross it, then emerge onto the $r < 0$ sheet keeping the same θ and φ values. The rays lying in the equatorial plane $\theta = \frac{1}{2}\pi$ are exceptions. These are tangent to the ring singularity at $\Sigma = 0$, meeting it after a finite lapse of affine parameter r .²²

It is not easy to detect the remaining principal null vector \mathbf{l} which is hidden in (2.7) or (2.15). Equation (2.13) offers a clue; it is invariant under the transformation $d\bar{r} \rightarrow -d\bar{r}$ which interchanges ingoing and outgoing rays. In system (S) , therefore, \mathbf{k} and \mathbf{l} differ only in the sign of their radial components. Applying the transformation (2.11) to \mathbf{k} gives us the following:

$$\mathbf{k} = (k^{\bar{r}}, k^{\bar{t}}, k^{\bar{\theta}}, k^{\bar{\varphi}}) \\ = [-1, 0, -a/\Delta, (r^2 + a^2)/\Delta] \quad (2.16b)$$

and consequently

$$\mathbf{l} = (l^{\bar{r}}, l^{\bar{t}}, l^{\bar{\theta}}, l^{\bar{\varphi}}) \\ = [+1, 0, -a/\Delta, (r^2 + a^2)/\Delta]. \quad (2.17b)$$

It is then a simple matter to determine the components of \mathbf{l} in the (E) frame:

$$\mathbf{l} = (l^r, l^t, l^\theta, l^\varphi) \\ = [+1, 0, -2a/\Delta, (r^2 + a^2 + 2mr)/\Delta]. \quad (2.17a)$$

Note that $\bar{r} = r$ is an affine parameter along *both* ray systems, but that t is an affine parameter only for the ingoing congruence.

Equation (2.17a) fails at the horizons $r = r_\pm$, but if we rewrite it as

$$\mathbf{l} = N(\Delta, 0, -2a, r^2 + a^2 + 2mr)$$

with N an unspecified normalization factor, we can take the limit $r \rightarrow r_\pm$ without difficulty. The result,

$$\mathbf{l}_\pm = N_\pm(0, 0, -2a, 4mr_\pm), \quad (2.18)$$

displays the key role of \mathbf{l}_\pm as the *null generators* of

²² This shows, incidentally, that the ring singularity is real, for it is easily seen that $d^2H/d\mu^2$, which is an algebraic invariant of the Riemann tensor [see Eq. (2.2a)], becomes infinite there.

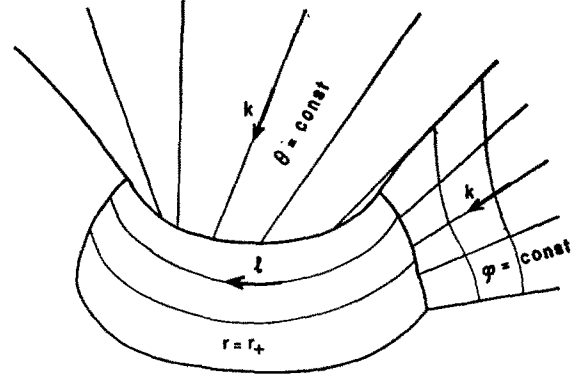


FIG. 3. The horizon $r = r_+$, viewed from the (M) frame with (x, y, z) as Cartesian coordinates. The principal null congruence \mathbf{l} lying in the horizon is shown, as well as portions of the \mathbf{k} congruence lying in the coordinate surface $\theta = \pi/4$ and $\varphi = \text{const}$.

the corresponding horizons (see Fig. 3). The affine parameter for this special case is not obvious—it evidently cannot be r , and it turns out that t does not work either—but we postpone this question until Sec. IV [see in particular Eq. (4.11)].

This result appears at first sight to violate the symmetry between the two principal null congruences. However, from Eq. (2.3b), there must exist another coordinate frame— (E') say—adapted to the \mathbf{l} congruence, in which the roles of \mathbf{k} and \mathbf{l} are interchanged. This frame is not hard to find. Using Eq. (2.11) as a guide, we make the obvious transformation

$$\bar{r} = r', \quad \bar{\theta} = \theta', \\ d\bar{\varphi} = d\varphi' - a dr'/\Delta, \quad (2.19) \\ d\bar{t} = dt' + 2mr' dr'/\Delta$$

and obtain a line element just like (2.7), except that the sign of dr (or equivalently, of $d\varphi$ and dt) is reversed:

$$ds^2 = dr'^2 - 2a \sin^2 \theta dr' d\varphi' \\ + (r'^2 + a^2) \sin^2 \theta d\varphi'^2 + \Sigma d\theta'^2 - dt'^2 \\ + (2mr'/\Sigma)(dr' - a \sin^2 \theta d\varphi' - dt')^2. \quad (2.20)$$

A further transformation, from (E') to the associated Minkowski (M') frame (x', y', z', t') , proceeds essentially via Eqs. (2.6), except that $\varphi = \tan^{-1}(a/r)$ is replaced by $\varphi' = \tan^{-1}(a/r)$. One finds

$$\mathbf{k} = (k^{r'}, k^{\theta'}, k^{\varphi'}, k^{t'}) \\ = [-1, 0, -2a/\Delta, (r'^2 + a^2 + 2mr')/\Delta], \quad (2.16c)$$

$$\mathbf{l} = (l^{r'}, l^{\theta'}, l^{\varphi'}, l^{t'}) = (+1, 0, 0, +1), \quad (2.17c)$$

which is just the reverse of (2.16a), (2.17a), as

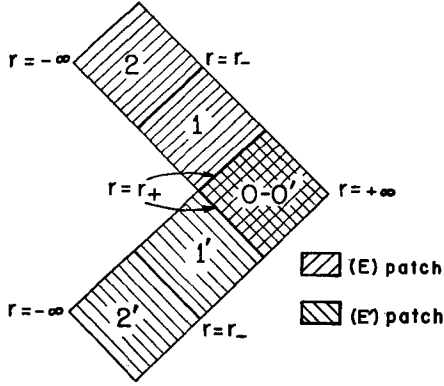


FIG. 4. The pair of (E) and (E') coordinate patches for the Kerr metric, drawn in a fashion roughly analogous to Fig. 1. Even-numbered regions, which are asymptotically flat, are separated by an odd-numbered interior region whose boundaries are the two horizons r_{\pm} . Although the drawing is only meant to be symbolic, the compression of the asymptotic regions is suggestive of a Penrose conformal transformation [R. Penrose, *Relativity, Groups and Topology*, B. DeWitt and C. DeWitt, Eds. (Gordon and Breach Science Publishers, New York, 1964)].

is to be expected. Note that in this frame it is the \mathbf{k} congruence which provides the generators for the horizons.

This result is not paradoxical, for the two coordinate frames are not equivalent. Combining Eqs. (2.11) and (2.19), one gets the direct transformation equations $(E) \rightarrow (E')$. For $a^2 > m^2$ this transformation is one-to-one over the entire range of r values, but for $a^2 \leq m^2$, which is the interesting case, the (E) and (E') coordinate patches only partially overlap. It is a straightforward matter to show that

$$t' = t - \frac{2m}{(m^2 - a^2)^{1/2}} \left[r_+ \ln \left| \frac{r - r_+}{2m} \right| - r_- \ln \left| \frac{r - r_-}{2m} \right| \right] \quad (2.21)$$

and

$$\varphi' = \varphi + \frac{a}{(m^2 - a^2)^{1/2}} \ln \left| \frac{r - r_+}{r - r_-} \right|,$$

from which it is clear that either (t, φ) or (t', φ') must diverge at r_{\pm} . We thus obtain three inequiva-

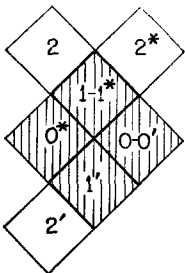


FIG. 5. The diagram of Fig. 4, enlarged by the addition of another (E') patch labeled $\{0^*, 1^*, 2^*\}$. The shaded portion defines the Kruskal or (K) patch.

lent analytic extensions of the original (E) frame, according as we choose r to lie in the different intervals $-\infty < r < r_-$, $r_- < r < r_+$, $r_+ < r < \infty$. Putting these several pieces together to make a smooth manifold is the job of the next section.

III. ANALYTIC EXTENSIONS

"Kruskal-Like" Coordinates

Let us mark the three domains $r > r_+$, $r_- < r < r_+$, $r < r_-$ within the (E) patch as regions $\{0, 1, 2\}$, respectively. Transforming from (E) to (E') via Eq. (2.21) we obtain three similar domains, $\{0', 1', 2'\}$. We assume that the transformation is one-to-one (and therefore analytic) between $\{0\}$ and $\{0'\}$; it then follows that $\{1\}$ and $\{1'\}$ are inequivalent—one has a boundary crossed by the \mathbf{k} congruence, the other by the \mathbf{l} congruence—and likewise for $\{2\}$ and $\{2'\}$. Putting the two patches together, we obtain the enlarged domain shown schematically in Fig. 4.

Now take another (E') patch, whose sections are labeled $\{0^*, 1^*, 2^*\}$, and tie it into the middle region of the original (E) patch, by requiring that the domains $\{1\}$ and $\{1^*\}$ coincide. The manifold has now grown to the size of Fig. 5.

We have drawn the two regions $\{0^*\}$ and $\{1^*\}$ as contiguous, but this is unfair, for there is no reason in the foregoing to suppose that they are in any way related. We now wish to demonstrate that the picture is in fact a reasonable one, by displaying a single coordinate system in which the four regions $\{0, 1, 0^*, 1^*\}$ are linked together as shown. Such a linkage looks very similar to a Kruskal diagram (Fig. 1). Our object, therefore, is to find a transformation analogous to (1.4), such that both segments of the horizon $r = r_+$ appear regular when viewed from these new coordinates.

The task is not a trivial one. For one thing, the principal null congruences of the Schwarzschild metric are straightened out in Kruskal coordinates to the lines $u \pm v = \text{const}$, $\theta, \varphi = \text{const}$. One might hope, by combining a transformation of the azimuthal angle with a suitable generalization of Eq. (1.4), to achieve a similar simplification here. But the corresponding vectors \mathbf{k} and \mathbf{l} of the Kerr metric are not in general 2-surface-forming, so that such a search is pointless. We settle for a frame in which the principal null rays merely lie in the surfaces $u \pm v = \text{const}$. This solution, while less elegant than Kruskal's, is adequate for our purposes, and is perhaps as close as one can come to a generalization of it.

Since we want to treat both congruences impar-

tially, we start from the (S) frame. From the expressions for \mathbf{k} and \mathbf{l} in these coordinates [Eqs. (2.16b), (2.17b)], it may be seen that as $r \rightarrow r_+$ both become asymptotic to a family of helices winding around the horizon, given by

$$dr: d\theta: d\bar{\varphi}: d\bar{t} = 0: 0: -a: 2mr_+.$$

We seek a transformation of the azimuthal coordinate which will straighten out the helices. Many obvious possibilities suggest themselves, but one encounters later difficulties unless one picks the new coordinate to be a linear combination of $\bar{\varphi}$ and \bar{t} with *constant* coefficients, plus any function of r and θ , and this restricts the choice to

$$w = \bar{\varphi} + (a/2mr_+)\bar{t} + \psi(r, \theta). \quad (3.1)$$

For simplicity we take $\psi(r, \theta) = 0$. It is quite possible that other choices might lead to a more tractable form for the metric; we have not investigated this in any detail.

Through Eq. (3.1) we have untwisted the null curves in the limit $r \rightarrow r_+$ (at the expense, incidentally, of twisting them in the neighborhood of spatial infinity, which may be disagreeable but is not serious—Kruskal-type coordinates are not at all well adapted to the asymptotically flat portions of the manifold anyway.) The metric computed from (2.13) after this single change of variables is still singular at r_+ , of course, but now we know how to deal with it. We make a further transformation $(r, t) \rightarrow (u, v)$, such that the integral curves of the two principal congruences lie in the hypersurfaces $u \pm v = \text{const}$, although not in $w = \text{const}$. According to Eqs. (2.16b), (2.17b), these integral curves satisfy

$$dr/\Delta(r) = \mp d\bar{t}/(r^2 + a^2),$$

or

$$\left(\frac{r-r_+}{2m}\right)\left(\frac{r-r_-}{2m}\right)^{-\nu} \exp\left(\frac{r \pm \bar{t}}{\sigma_+}\right) = \text{const} = F(u \pm v), \quad (3.2)$$

with

$$\sigma_{\pm} \equiv mr_+(m^2 - a^2)^{-1/2} \quad (3.3)$$

and

$$\nu \equiv r_-/r_+.$$

From the work of Kruskal and Graves-Brill we are led to take²³ $F(x) = x^2$, and consequently

$$u \pm v = \left(\frac{r-r_+}{2m}\right)^{1/2} \left(\frac{r-r_-}{2m}\right)^{-\nu/2} \exp\left(\frac{r \pm \bar{t}}{2\sigma_+}\right). \quad (3.4)$$

²³ Had we wanted the transformation to yield a metric regular across r_- , the appropriate choice would have been $F(x) = x^{-2\nu}$.

Although this is only defined for $r > r_+$, \bar{t} finite (i.e., for $u > |v|$), the inverse transformation, given implicitly by

$$\Psi(r) \equiv \left(\frac{r-r_+}{2m}\right)\left(\frac{r-r_-}{2m}\right)^{-\nu} e^{r/\sigma_+} = u^2 - v^2 \quad (3.5)$$

and

$$\bar{t} = \sigma_+ \tanh^{-1} [2uv/(u^2 + v^2)]$$

is well defined over the cut plane $u^2 \neq v^2$. In particular, $\Psi(r)$ increases monotonically from $-\infty$ to 0 to $+\infty$ as r runs from r_- to r_+ to $+\infty$, and is an analytic function of r over this interval, so that $r(u, v)$ is an analytic function over the u, v plane, while $\bar{t}(u, v)$ diverges at $u = \pm v$ and is analytic elsewhere. As the coordinates (u, v, w, θ) —which we henceforth call the (K) frame—vary over their respective ranges

$$-\infty < u < \infty, \quad -\infty < v < \infty, \\ 0 \leq w < 2\pi, \quad 0 \leq \theta \leq \pi$$

they cover the four regions $\{0, 1, 1' \text{ and } 0^*\}$ of Fig. 5; the boundaries between adjacent regions are the pair of lines $u = \pm v$ on which $r = r_+$. Note that region $\{0^*\}$, in which $u < |v|$ (and therefore $r > r_+$), forms the second sheet of an Einstein-Rosen bridge.

In the following it is convenient to know the direct transformation from (E) to (K) coordinates. This is given by

$$u + v = e^{(r+t)/2\sigma_+}, \\ u - v = \Psi(r)e^{-(r+t)/2\sigma_+}, \quad (3.6) \\ w = \varphi + \left(\frac{a}{2mr_+}\right)t - \frac{a}{r_+} \ln \left(\frac{r-r_-}{2m}\right).$$

The transformation from (E') to (K) is obtained similarly, with t replaced by $-t'$. Equation (3.6) evidently defines an analytic homeomorphism of the domain $r > r_+$, $-\infty < t < \infty$ onto the half-plane $u + v > 0$, i.e., onto the region $\{0, 1\}$.

On the other hand, we could have mapped the domain $-\infty < r < r_+$, $-\infty < t < \infty$ homeomorphically into a (different) Kruskal patch by regularizing about the other event horizon, $r = r_-$.²³ The latter transformation, $(E) \rightarrow (K')$ say, takes the form

$$u' + v' = -e^{-(r+t)/2\sigma_-}, \\ u' - v' = -\left(\frac{r_- - r}{2m}\right)\left(\frac{r_+ - r}{2m}\right)^{-1/\nu} e^{-(r-t)/2\sigma_-}, \quad (3.7) \\ w' = \varphi + \left(\frac{a}{2mr_-}\right)t - \frac{a}{r_-} \ln \left(\frac{r_+ - r}{2m}\right).$$

We postpone a discussion of the full import of this result until later in the section, in order to settle a fundamental point.

Analyticity of the Metric in (K) Coordinates

There remains the very important but rather tedious job of working out the components of the Kerr metric in (K) coordinates, and demonstrating that they are indeed analytic functions of u and v throughout the (u, v) plane. We spare you the details, and merely assert that after much labor one can cast the metric in the following form:

$$\begin{aligned} ds^2 = & \Sigma d\theta^2 + 4\sigma_+^2 \Sigma (r^2 + a^2)^{-2} (du^2 - dv^2) \\ & + \Sigma^{-1} \sin^2 \theta [(r^2 + a^2) dw + a(m^2 - a^2)^{-1/2} f \\ & \times (r + r_+)(r - r_-)^{-1} (v du - u dv)]^2 \\ & + (\Sigma \Delta)^{-1} \{ [2\sigma_+ f \Sigma (r^2 + a^2)^{-1} (v du - u dv)]^2 \\ & - [2\sigma_+ f \Sigma_+ (r_+^2 + a^2)^{-1} (v du - u dv) \\ & - a \sin^2 \theta \Delta dw]^2 \}. \end{aligned} \quad (3.8)$$

Here we have introduced

$$\Sigma_{\pm} = \Sigma(r_{\pm}, \theta) \quad (3.9a)$$

and

$$\begin{aligned} f(r) &= \Delta(r)/\Psi(r) \\ &= 4m^2 [(r - r_-)/2m]^{2m/r_+} e^{-r/a_+}. \end{aligned} \quad (3.9b)$$

Since Σ and f are both analytic and nonzero throughout the whole (u, v) plane, it is clear that only the term in (3.8) with $\Delta(r)$ in the denominator can lead to difficulty. Closer inspection shows, however, that the numerator of this term has a simple zero at $r = r_+$ also, so the quotient remains analytic.

Had we chosen to regularize across r_- instead, using Eq. (3.7) or its equivalent, we would have obtained much the same result, except for the inevitable branch point at $r(u, v) = 0$ and $\theta = \frac{1}{2}\pi$.

The line element (3.8) is much too cumbersome to be of any direct use. Fortunately, once we have established its analyticity we need make no further use of it. This is to some extent regrettable, for it

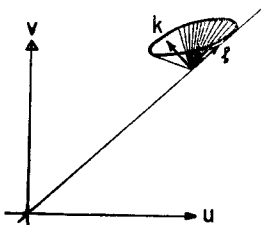


FIG. 6. The null cone at a point in the horizon $r = r_+$. The cone is lopsided and spills out of the angle defined by the principal null vectors k and l ; in addition, the shaded portion of the cone behind the (u, v) plane is smaller than the portion jutting out in front of it. Although the shape of the cone varies from point to point, the projections of k and l onto the plane always have slope ± 1 .

would have been desirable to have a coordinate system in which, like Kruskal's, the null curves took an especially simple form (see Fig. 6). Cohen and Brill,²⁴ in their study of metrics for slowly rotating bodies, have applied the Kruskal procedure to a line element differing from the Schwarzschild form by terms of first order in the angular velocity. We recover their results if we drop from Eq. (3.8) all terms of order a^2 ; this leaves

$$\begin{aligned} ds^2 \simeq & r^2 (d\theta^2 + \sin^2 \theta dw^2) \\ & + (32m^3/r) e^{-r/2m} (du^2 - dv^2) \\ & + (4a/r) \sin^2 \theta e^{-r/2m} \\ & \times (r^2 + 2mr + 4m^2) dw (v du - u dv). \end{aligned} \quad (3.10)$$

To this order, the curves $u \pm v = \text{const}$, $w, \theta = \text{const}$ are null, just as in the Kruskal form of the Schwarzschild metric.

Construction of a Maximal Analytic Manifold

What we have done to extend the domain $\{0, 1\}$ we can also do to the domain $\{1, 2\}$. We use the alternative transformation (3.7) to produce a new (K') patch, consisting of the three regions $\{1, 2, 2^*\}$ already introduced plus a new domain $\{3\}$, which, like $\{1\}$, is bounded by two pairs of horizons (see Fig. 7). Here also the asymptotically flat portions, $\{2\}$ and $\{2^*\}$, form two sheets of an Einstein-Rosen bridge. While isometric to each other, these are not isometric to $\{0\}$ and $\{0^*\}$ —they have, it may be recalled, the sort of geometry one would associate with a negative mass source.

A similar extension can be applied to the domain $\{1', 2'\}$. In view of the picture which is rapidly emerging, we find it preferable to change our notation slightly, and to write $\{-1, -2\}$ instead of $\{1', 2'\}$. Thus the new Kruskal patch encompasses the regions $\{-1, -2, -2^*, -3\}$ of Fig. 7.

This procedure can clearly be continued indefinitely in both directions, and generates an infinite chain of overlapping (E) and (E') patches. The result can be viewed even more simply as a chain of overlapping "Kruskal" patches, $\{K_n\}$, isometric to (K) or (K') according as n is even or odd. We can, in fact, eliminate any reference whatever to the auxiliary (E) and (E') frames, by presenting the transformation equations that connect (K) and (K') ; these take the surprisingly simple form

$$\begin{aligned} (u + v)^{r_+} (-u' - v')^{r_-} &= 1, \\ (-u + v)^{r_+} (u' - v')^{r_-} &= 1, \end{aligned} \quad (3.11a)$$

²⁴ D. R. Brill and J. M. Cohen, Phys. Rev. **143**, 1011 (1966).

and

$$\begin{aligned} w' - w &= (2a/r_-) \ln [(u + v)/(-u + v)] \\ &= -(2a/r_+) \ln [(u' - v')/(-u' - v')]. \end{aligned} \quad (3.11b)$$

These transformations are one-to-one and analytic in the domains $\dots \{1\}, \{3\}, \dots$ of overlap, and have the following simple properties: They preserve straight lines of slope ± 1 as well as the straight lines $v/u = \text{const}$ and the hyperbolas $v^2 - u^2 = \text{const}$, while mapping the north quadrant of (K) onto the south quadrant of (K') .

The manifold we have constructed has many curious properties. It has infinitely many disjoint and asymptotically flat sheets, for one thing, and therefore does not admit a Cauchy surface. In fact, one can get from any such even-numbered sheet to any other—with the sole exception of the companion sheet on the other side of the “bridge”—by following a suitable timelike or lightlike curve. The timelike curve $u = 0 (u' = 0)$, $w, \theta = \text{const}$ is particularly noteworthy, for it defines the location of the “throat” of an Einstein-Rosen bridge. The throat itself (i.e., the 2-surface $u = 0, v = \text{const}$) has an area which pulsates with time, in close analogy with the Reissner-Nordström case.¹² Since the throat is deformed, due to the effects of rotation, its area is no longer given by the simple formula $4\pi r^2$ obtained for the Schwarzschild and Reissner-Nordström metrics, but by the more complicated expression

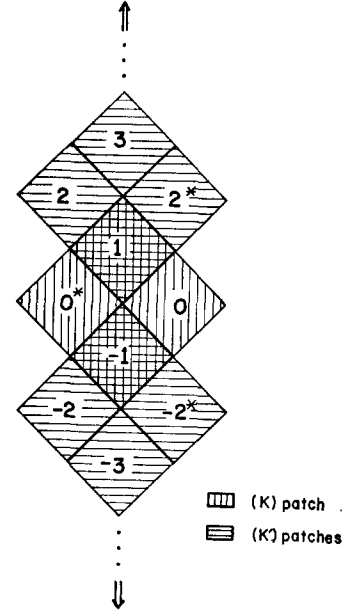
$$\begin{aligned} \text{area} &= 2\pi(r^2 + a^2) \\ &+ (g/a)(-\Delta)^{-\frac{1}{2}} \sin^{-1} [a(-\Delta/g)^{\frac{1}{2}}] \end{aligned} \quad (3.12)$$

with $g(r) = (r^2 + a^2)^2 - a^2\Delta$. At the horizons $r = r_{\pm}$, where the extrema occur, this simplifies to

$$\text{area}_{\pm} = 8\pi m r_{\pm}. \quad (3.12)$$

The manifold sketched in Fig. 7 is not the only possible maximal extension, because of the freedom still remaining to make topological identifications. The simplest manifold of this more general type arises if we identify $\{K_{2n}\}$ with $\{K_{2n+4}\}$. It is covered by only two Kruskal patches, $\{K_0\}$ and $\{K_2\}$ say, with regions $\{-1\}$ and $\{3\}$ identified, so it consists of four asymptotically flat sheets (two with positive mass, two negative) glued together with two interior regions.²⁵ This manifold, like the others obtained in the same way, is violently acausal—a properly aimed signal will emerge, after crossing four hori-

FIG. 7. A chain of Kruskal patches, with those of (K) and (K') type alternating and partially overlapping. The complete figure extends indefinitely in both directions, to form a maximal analytic extension of the Kerr manifold.



zons, in the past light cone of the source which emitted it—and this may be felt to be a bit unrealistic.²⁶

The foregoing construction presupposes, of course, that the metric admits two distinct horizons. For $a^2 > m^2$ the horizons disappear and the transformation to Kruskal coordinates loses all meaning; all that remains are two asymptotically flat spaces joined at the disk $r = 0$. The exceptional case $|a| = m$ deserves special comment. Carter has studied this in detail¹⁶; although his work was confined to the symmetry axis ($\theta = 0, \pi$), it is clear that his conclusions apply with equal force to the full metric: One builds up a ladder of alternating (E) and (E') patches (with or without identifications) in the simple sequence $\{\dots - 2, 0, 2, \dots\}$. The odd-numbered sheets disappear; there is nothing to correspond to the second Kruskal sheets $\{\dots - 2^*, 0^*, 2^*, \dots\}$; and in fact there is no need at all to introduce (K) -type coordinates to cover the manifold in this case.

IV. GEODESIC COMPLETENESS

Geodesic Equations, First Integrals

For the study of geodesics the original (E) coordinates are particularly convenient. Let μ be an affine path parameter, normalized to give proper time along timelike geodesics, and use a dot to

²⁵ This particular choice was made by Graves and Brill.¹² It is clear from their work, however, that the identification is unnecessary; one can also describe the Reissner-Nordström metric by an infinite chain of Kruskal patches.

²⁶ B. Carter has pointed out that for small negative values of r and values of θ near the equator $g_{\varphi\varphi}$ goes negative. Hence as long as one adopts a topology in which φ is treated as an angular coordinate there will necessarily exist closed timelike curves in this region.

denote differentiation with respect to μ . The geodesic equations can be extracted in the usual way from the variational principle $\delta \int L d\mu = 0$, with a Lagrange function given by

$$2L = \dot{r}^2 + 2a \sin^2 \theta \dot{\phi} + (\dot{r}^2 + a^2) \sin^2 \theta \dot{\phi}^2 + \Sigma \dot{\theta}^2 - \dot{t}^2 + (2mr/\Sigma)(\dot{r} + a \sin^2 \theta \dot{\phi} + \dot{t})^2 \quad (4.1)$$

as in Eq. (2.7).

We are chiefly interested not in the equations of motion themselves, but rather in their first integrals. Since φ and t are cyclic, we obtain two integrals immediately:

$$\begin{aligned} p_\varphi &\equiv \partial L / \partial \dot{\phi} = l, \\ p_t &\equiv \partial L / \partial \dot{t} = -\gamma, \end{aligned} \quad (4.2a)$$

with l and γ representing the angular momentum/mass and energy/mass of a test particle moving along the given geodesic. (On null geodesics μ is defined only up to a linear transformation, and consequently only the ratio l/γ is meaningful. We remove the arbitrariness by taking $\gamma = 1$ in this case.) A third integral is given by L itself:

$$2L = -\epsilon, \quad (4.2b)$$

the indicator ϵ being $+1, 0, -1$ for timelike, null, and spacelike geodesics, respectively.

The remaining two conjugate momenta are readily found to be

$$\begin{aligned} p_r &= (\Sigma \dot{r} + al + 2mr\gamma)/\Delta, \\ p_\theta &= \Sigma \dot{\theta}, \end{aligned} \quad (4.3)$$

which shows, incidentally, that we can expect difficulties with the equations of motion at the ring singularity ($\Sigma = 0$) and at the horizons ($\Delta = 0$). It is clear from the form of L that $p_\theta = 0$ is consistent with the equations of motion if $\theta = 0$ or π (axial case) or if $\theta = \frac{1}{2}\pi$ (equatorial case); in these special cases the first integrals (4.2) yield a complete solution by quadratures, which we consider in greater detail in Sec. V.

From Eq. (4.2a) we can express $\dot{\phi}$ and \dot{t} in terms of \dot{r} and the constants of integration; the resulting formulas are

$$\begin{aligned} \dot{\phi} &= \Sigma^{-1}[(l/\sin^2 \theta) - ap_r], \\ \dot{t} &= \Sigma^{-1}[\gamma(\Sigma + 2mr) + 2mrp_r], \end{aligned} \quad (4.4)$$

with p_r given by (4.3).

We note also the following form of Eq. (4.2b), which is important in later arguments:

$$\begin{aligned} \Sigma^2 \dot{r}^2 - (al + 2mr\gamma)^2 \\ = \Delta[-\epsilon\Sigma + (\Sigma + 2mr)\gamma^2 - p_\theta^2 - (l^2/\sin^2 \theta)]. \end{aligned} \quad (4.5)$$

Problem of Completeness

The Kerr metric evidently cannot be imbedded isometrically in a complete analytic manifold, since there exist geodesics—the principal null rays lying in the equatorial plane, for example—which strike the ring singularity at finite values of their affine parameters. If one excludes all such geodesics, it is reasonable to ask whether the remainder can be continued to arbitrarily large values of μ . We argue below that this is so, provided that the manifold is chosen to be the analytic extension described previously. In this sense, therefore, the extension can be regarded as maximal.

Since it is impossible to solve the geodesic equations exactly, except in a few very special cases, we base the argument on the first integrals (4.4) and (4.5). Starting with any set of initial values, one extends the solution either until a singular point is reached, or until one or more coordinates diverge. There is clearly no problem if r diverges—since the metric is asymptotically flat and therefore complete for $r \rightarrow \pm\infty$ —but only if $\dot{\phi}$, \dot{t} , or $\dot{\theta}$ diverge at finite values of r . As one sees from the above equations, this happens at $\Sigma = 0$, $\sin \theta = 0$ or $\Delta = 0$. If the first possibility occurs nothing can be done about it; the second is obviously a consequence of the spheroidal-type coordinates here employed, and can be eliminated by transforming to those of the (M) type. Thus it is only the apparent divergence of $\dot{\phi}$ and \dot{t} at the horizons that needs to be examined carefully. [It follows from Eq. (4.5) that \dot{r} remains finite at r_\pm ; the same is true of $\dot{\theta}$.] In fact, $\dot{\phi}$ and \dot{t} diverge if and only if p_r diverges, and it is easy to see that this happens if and only if \dot{r}_\pm has the same sign as $al + 2mr_\pm\gamma$, for Eqs. (4.3) and (4.5) imply

$$p_r = \frac{-\epsilon\Sigma + (\Sigma + 2mr)\gamma^2 - p_\theta^2 - (l^2/\sin^2 \theta)}{\Sigma\dot{r} - (al + 2mr\gamma)}, \quad (4.6)$$

which yields a finite limit whenever \dot{r}_\pm and $(al + 2mr_\pm\gamma)$ have opposite sign—that is, whenever the geodesic is ingoing. [Some confusion over the meaning of the term “ingoing” can arise here, unless one is careful. On the positive r sheet the hypersurfaces $t = \text{const}$ are everywhere spacelike: $(\text{grad } t)^2 = -1 - 2mr/\Sigma$, which is certainly negative for $r > 0$. Hence an ingoing path is properly defined as one

for which $dr/dt < 0$. For some values of l and γ Eqs. (4.3), (4.4) suggest that $dr/d\mu$ is positive on an ingoing path, but this simply means that the affine parameter has been chosen to increase into the past.]

We therefore conclude that all ingoing paths can be continued across the horizons. Some subsequently strike the ring singularity, others continue on to $r = -\infty$ (and are thus complete), a third class reaches a turning point and start back. On the return trip, however, both t and ϕ diverge as the horizon is approached. This is not surprising; the particle has merely run off the (E) coordinate patch. To continue to follow its motion transform to an (E') system, or equivalently to an appropriate set of (K) coordinates. It is clear that a result similar to Eq. (4.6) must also apply to the outgoing trajectory in this case; hence the particle re-emerges into an asymptotically flat "universe," but of course on a sheet different from the first. If the effective total energy $\Gamma \equiv \gamma^2 - \epsilon$ is positive, the particle escapes to infinity; if negative, it reaches another turning point and starts back toward $r = r_+$ again, in which case we transform to another set of (E) coordinates and repeat the cycle. Clearly μ can be made as large as we please by piecing together sufficiently many such cycles, which proves completeness for this case.

Of course there are many geodesics which do not fall into any of the above categories, such as the ones which oscillate to and fro between a maximum and minimum radius outside r_+ , and those which spiral in towards (or out from) an unstable circular orbit. However, these lead in general to no difficulties with completeness, since t remains finite as t increases to infinity.

There remains one further class to be considered, namely, the geodesics for which $\dot{r} = 0$ at r_{\pm} , or equivalently, for which

$$al = 2mr_{\pm}\gamma. \quad (4.7)$$

This class includes spacelike geodesics tangent to the horizons (these present no problems), geodesics of all three types which approach the horizon asymptotically as $t \rightarrow \pm\infty$, and finally, and most importantly, the principal null geodesics that are the generators of the horizons. We study the latter in detail below.

Completeness within the Horizons

To obtain the solution for the principal null ray 1 lying in r_{\pm} set $\Delta = 0$, $\epsilon = 0$ and also

$$\dot{\theta} = 0, \quad \gamma = l = 0. \quad (4.8)$$

The first integrals (4.5), (4.6) then yield the common solution

$$\dot{\phi} = -(a/2mr_{\pm})\dot{t} \quad (4.9)$$

in agreement with Eq. (2.18). To find $t(\mu)$ it is necessary to solve one of the geodesic equations, and the simplest to use is $\dot{p}_r = \partial L / \partial r$. A straightforward computation gives

$$\ddot{t} = \mp (2\sigma_{\pm})^{-1} \dot{t}^2,$$

with σ_{\pm} defined by Eq. (3.3). Hence

$$t(\mu) = \pm 2\sigma_{\pm} \ln(\mu - \mu_0) \quad (4.10a)$$

or

$$\mu - \mu_0 = e^{\pm t/2\sigma_{\pm}}. \quad (4.10b)$$

We emphasize that this result is exact.

On the event horizon $r = r_+$, $\mu \rightarrow +\infty$ as $t \rightarrow +\infty$, while $\mu \rightarrow \mu_0$ as $t \rightarrow -\infty$. This is just what one would have expected, since the (E) coordinates are known to be incomplete at r_+ for $t \rightarrow -\infty$. A full picture of the horizon $r = r_+$ is provided by viewing it in (K) coordinates; then the path equations become

$$u(\mu) = v(\mu) = \frac{1}{2}(\mu - \mu_0)e^{r_+/2\sigma_+}, \quad w(\mu) = \text{const} \quad (4.11)$$

and are evidently complete. A similar result applies at $r = r_-$, but with the time directions reversed; this too is consistent with the complete picture of this horizon when viewed from (K') coordinates (as in Fig. 7).

Qualitatively similar results emerge when one analyzes the geodesics that approach r_{\pm} asymptotically (i.e., as $t \rightarrow \pm\infty$). All timelike curves of this type reach a vertex such as $u = v = 0$ in a finite proper time and can be extended without difficulty; similar remarks apply to the null curves. There are others, necessarily spacelike, which approach r_+ from region $\{1\}$ as $t \rightarrow +\infty$ (or r_- as $t \rightarrow -\infty$), and these are in fact complete.

V. Equatorial Geodesics

The first integrals obtained in the previous section yield a complete description when $\theta = 0$ or π or when $\theta = \frac{1}{2}\pi$. The former case, which corresponds to motion along the symmetry axis, has been investigated by Carter¹⁶; we confine our attention, therefore, to the latter. Boyer and Price²⁰ have shown that the orbit equation for equatorial geodesics leads to a precession of the pericenter in agreement, through third order, with the approximate

calculations of Lense-Thirring. In the present section we concentrate on the qualitative features of geodesics in the strong field regions. Our analysis is patterned after the study of orbits in the Schwarzschild metric first carried out by Darwin²⁷ and later extended by Mielnik and Plebański.²⁸ Of course, all these studies are largely academic exercises, since in realistic situations (except possibly the late phases of gravitational collapse³) the geometry in these regions, and hence the geodesics themselves, differ considerably from the empty-space results, due to the nonzero stress-energy tensor there. Nevertheless, the study of the Kerr metric, even as an ideal case, has, we believe, some real value, for it helps to clarify the role which angular momentum plays in general relativistic models. In particular, because the character of the orbits in the interior regions changes markedly as soon as the central body is given some angular momentum, it seems worthwhile to point out those features of Darwin's analysis which are unique to the Schwarzschild problem, and those which persist in the $a \neq 0$ case as well.

Null Geodesics

It is simplest, and most instructive, to begin with the null rays. We normalize the affine parameter along the rays by taking $\gamma = 1$. Then the energy integral (4.5) reduces to

$$\dot{r}^2 = 1 + (a^2 - l^2)r^{-2} + 2m(a + l^2)r^{-3}. \quad (5.1)$$

For convenience set $\beta = 2m$ and introduce the dimensionless variables

$$\rho = r/\beta, \quad \lambda = l/\beta, \quad \alpha = a/\beta. \quad (5.2)$$

From (5.1) it is clear that turning points occur at the zeros of the cubic polynomial

$$\psi(\rho) = \rho^3 + (\alpha^2 - \lambda^2)\rho + (\alpha + \lambda)^2. \quad (5.3)$$

The location of these zeros is thus fundamental to a qualitative understanding of the null trajectories.

Applying the rule of signs, we see that $\psi(\rho) = 0$ has always one real negative root: a ray sent in from $r = -\infty$ is thus repelled and ultimately deflected back to $-\infty$. (The outgoing principal null ray, with $\lambda = -\alpha$, is an exceptional case; it alone strikes the $r = 0$ singularity from this direction.) On the positive sheet there are consequently either zero or two turning points, depending on the relative magni-

tudes of α and λ . If $\lambda^2 < \alpha^2$ there are clearly no real positive roots, so collapse to the singularity inevitably occurs. Conversely, if λ^2 is sufficiently large, incoming rays reach a pericenter and return to infinity, while outgoing rays from $r = 0$ reach an apocenter and fall back in. Thus one expects that there should exist two critical impact parameters, $\lambda_1 > 0$ and $\lambda_2 < 0$ say, such that light signals spiral in to $r = 0$ if $\lambda_2 < \lambda < \lambda_1$, and "bounce" back out to infinity otherwise. At these critical values of λ , $\psi(\rho)$ has a double zero, which defines the corresponding critical radii ρ_1, ρ_2 . A light ray at such a radius, and with the correct value for λ , will travel around in a circular orbit indefinitely, but such an orbit is, of course, unstable.

These predictions are borne out in the Schwarzschild case by Darwin's analysis. There, it may be recalled, the critical radii are both located at $\rho = \frac{3}{2}$ (or $r = 3m$), and the critical impact parameters are $\lambda = \pm 3(\frac{3}{2})^{1/2}$. Most importantly, there do not exist any light rays whose pericenters lie inside $r = 3m$. If one imagines the parameter α (or a) being increased gradually from zero, one expects $\rho_1(\alpha)$ and $\rho_2(\alpha)$ to depart smoothly from the Darwin value, and this is precisely what happens. In fact, one can give fairly simple closed expressions for the critical radii. These must be double zeros of $\psi(\rho)$ and thus must satisfy the condition

$$\rho(\rho - \frac{3}{2})^2 - 2\alpha = 0.$$

Solving this by standard methods, one finds²⁹

$$\begin{aligned} \rho_1 &= \frac{3}{2} + \alpha \sec(\frac{1}{3} \cos^{-1} 2\alpha), \\ \rho_2 &= \frac{3}{2} + \alpha \sec(\frac{1}{3} \cos^{-1} 2\alpha + \frac{2}{3}\pi), \end{aligned} \quad (5.4a)$$

provided that $\alpha \leq \frac{1}{2}$; there is only one critical radius, at

$$\rho_1 = \frac{3}{2} + \alpha \operatorname{sech}(\frac{1}{3} \cosh^{-1} 2\alpha), \quad (5.4b)$$

if $\alpha > \frac{1}{2}$. (Note that ρ_1 is always larger than ρ_2 . This is to be expected, since the centrifugal barrier is stronger if λ is positive.)

However, when $\alpha \neq 0$ a completely novel feature emerges: for a small range of impact parameters, $\lambda_3 \leq \lambda < -\alpha$, pericenters exist *inside the inner horizons*, and, in fact, for all values of ρ between 0 and ρ_- . This remarkable property permits one to transmit information from one positive sheet to another by bouncing a light signal off a centrifugal barrier inside ρ_- .

²⁷ C. Darwin, Proc. Roy. Soc. (London) **A249**, 180 (1959); **A263**, 39 (1961).

²⁸ B. Mielnik and J. Plebański, Acta Phys. Polon. **21**, 239 (1962).

²⁹ A third zero, $\rho_3 = \frac{3}{2} + \alpha \sec(\frac{1}{3} \cos^{-1} 2\alpha - \frac{2}{3}\pi)$, has a somewhat different interpretation: it describes the maximum possible apocenter within the inner horizon.

This result is illustrated by Fig. 8, which shows the portion of the λ - ρ plane in which light trajectories are possible. The boundary curve separating allowed and forbidden regions is obtained from Eq. (5.3) with $\psi(\rho) = 0$; it is given in explicit form as

$$\lambda = (1 - \rho)^{-1} \{-\alpha \pm \rho[(\rho - \rho_+)(\rho - \rho_-)]^{\frac{1}{2}}\}. \quad (5.5)$$

Not surprisingly, the shape of this curve is qualitatively different in the two cases $\alpha < \frac{1}{2}$ (where horizons exist) and $\alpha > \frac{1}{2}$ (where they do not). In the latter case pericenters occur in the region $\rho > \rho_1$ for λ positive [with ρ_1 given by Eq. (5.4b)], and over the entire region $\rho > 0$ for λ negative.

Timelike Geodesics

A very similar analysis can be carried through for the timelike geodesics; it is complicated, however, by the presence of an additional energy parameter, $p_t = -\gamma$ or equivalently $\Gamma = \gamma^2 - 1$, which governs the type of motion that results. In the Schwarzschild case, it may be recalled, the minimum possible pericenter for a particle trajectory changes with the effective total energy Γ in the fashion shown by Fig. 9. There are no pericenters for $\rho < \frac{3}{2}$. To reach a point between $\frac{3}{2} < \rho < 2$ and be deflected back out again the particle must come from infinity with

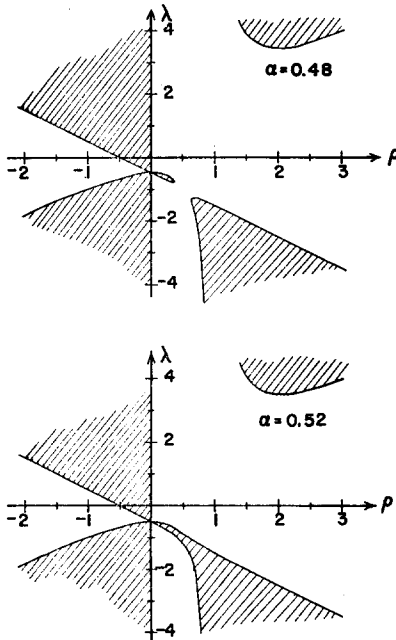


FIG. 8. A diagram of the λ - ρ plane, showing the regions in which light trajectories can exist. Shaded regions are forbidden; their boundaries define the turning points for null rays. Two cases, $\alpha = 0.48$ and $\alpha = 0.52$, are shown; the former contains horizons, at $\rho_- = 0.36$ and $\rho_+ = 0.64$. Note the small forbidden region extending from $\rho = 0$ to $\rho = \rho_-$ when λ is negative in the former case. When $\alpha \geq \frac{1}{2}$ the two forbidden regions for $\lambda < 0$ coalesce.

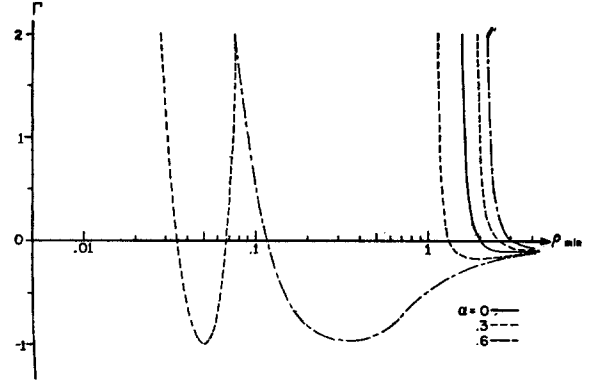


FIG. 9. Minimum pericenter for timelike geodesics as a function of effective total energy Γ , shown for $\alpha = 0, .3, .6$. The graph for $\alpha = 0.3$ has three components, corresponding to $\lambda < 0, \rho < \rho_-, \lambda < 0$, and $\rho > \rho_+, \lambda > 0$; that for $\alpha = 0.6$ has two components, corresponding to $\lambda < 0$ and $\lambda > 0$. Note that the $\rho < \rho_-$ portion (when it exists) covers the entire available energy range $\Gamma \geq -1$. Stable bound orbits in the exterior region occur for $\rho > \rho_{\text{orbit}}$, where ρ_{orbit} is the value of ρ at which the graph has zero slope—see also Fig. 11.

positive energy. At $\rho = 2$ the required total energy is zero, and it decreases to a minimum value of $\Gamma = -\frac{1}{3}$ at $\rho = 3$ (or $r = 6m$). These features are reflected in the stability of circular orbits: they are stable if and only if ρ exceeds 3. We therefore recognize in the Schwarzschild problem three characteristic radii—in addition to the famous “singularity” at $\rho = 1$ —given by $\rho = \frac{3}{2}, 2$, and 3. Let us try to determine the corresponding characteristic radii in the Kerr metric.

First of all, the minimum pericenters analogous to $\rho = \frac{3}{2}$ are given once more by Eqs. (5.4a) or (5.4b). But the striking feature of the null case persists here as well: at all energies (i.e., for all $\Gamma \geq -1$) pericenters are found within the region $0 < \rho \leq \rho_-$, so that these minima are not absolute ones if α differs from zero.

To see how the character of the motion changes as Γ is varied, a diagram of the λ - ρ plane, showing allowed and forbidden regions for various values of Γ , may again be helpful (see Fig. 10). The turning points, which separate these two regions, are still given by the zeros of a cubic polynomial:

$$\psi(\rho) \equiv \Gamma \rho^3 + \rho^2 + (\Gamma \alpha^2 - \lambda^2) \rho + (\lambda + \gamma \alpha)^2. \quad (5.6)$$

Solved explicitly for λ , this gives

$$\lambda = (1 - \rho)^{-1} \{-\gamma \alpha \pm [\rho(\rho - \rho_+)(\rho - \rho_-)(\Gamma \rho + 1)]^{\frac{1}{2}}\}, \quad (5.7)$$

analogous to Eq. (5.5). By studying the double zeros of $\psi(\rho)$ one constructs the plot of Γ vs minimum pericenter shown in Fig. 9. The critical energy corresponding to Darwin's value $\Gamma_{\text{crit}} = -\frac{1}{3}$ splits into

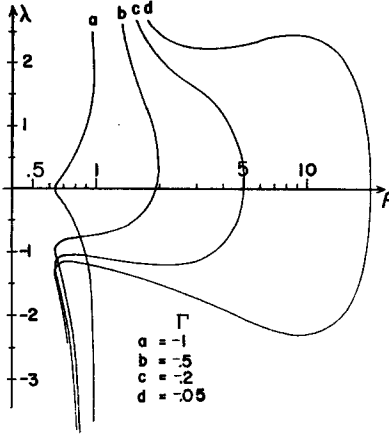


FIG. 10. A portion of the λ - ρ plane (cf. Fig. 8), showing regions in which timelike trajectories can exist. Graphs were plotted for $\alpha = 0.48$ and for several values of $\Gamma < 0$. In each case the allowed region lies to the left of the curve. An additional forbidden region, not shown on the graph, extends from $\rho = 0$ to $\rho = \rho_{\text{crit}}$, much like the one shown in Fig. 8. Allowed regions also exist on the negative sheet for $\Gamma > 0$. Graphs (a) and (b) illustrate the case of no bound orbits; (c) has bound orbits for $\lambda < 0$, (d) for $\lambda > 0$ as well.

two values, $\Gamma_{\text{crit}}^{\pm}$, say. As Fig. 10 makes clear, stable bound orbits in the exterior region are possible if $\Gamma_{\text{crit}}^{-} < \Gamma < 0$ and λ is negative; if $\Gamma_{\text{crit}}^{+} < \Gamma < 0$, they are possible for positive λ as well.

It is easy to see that Γ attains these critical values whenever the cubic polynomial $\tilde{\psi}(\rho)$ has a triple zero. Consequently,

$$\Gamma_{\text{crit}} = -1/(3\rho_{\text{crit}}) \quad (5.8a)$$

with ρ_{crit} in turn a real root of the following quartic:

$$\rho^4 - 6\rho^3 + (9 - 6\alpha^2)\rho^2 - 14\alpha^2\rho + 9\alpha^4 = 0. \quad (5.8b)$$

There are in general two such roots, with corresponding critical energies $\Gamma_{\text{crit}}^{\pm}$, shown in Fig. 11.

Exact Solutions; The Deflection of Light

The above work is based almost exclusively on the energy integral, Eq. (4.5). This does not differ substantially from the corresponding formula in the Schwarzschild problem—at least, not as long as one restricts his attention to the equatorial plane—so that the solution for $r(\mu)$ should be basically the same. Indeed, on making the standard transformation $u = 1/r$ one gets

$$u^2 = u^4 B(u) \quad (5.9a)$$

with $B(u)$ a cubic polynomial:

$$B(u) = \Gamma + \epsilon\beta u + (\Gamma a^2 - l^2)u^2 + \beta(l + \gamma a)^2 u^3. \quad (5.9b)$$

Hence $u(\mu)$ can be expressed in terms of elliptic functions. The other first integrals, for $\dot{\phi}$ and \dot{t} ,

do not yield so easily; however, the orbit equation is again relatively simple. One finds²⁰

$$\frac{d\phi}{du} = \frac{a}{D(u)} \pm \frac{A(u)}{D(u)[B(u)]^{\frac{1}{2}}} \quad (5.10)$$

with $B(u)$ defined as above, and

$$A(u) = l - \beta(l + \gamma a)u,$$

$$D(u) = 1 - \beta u + a^2 u^2 \equiv a^2(u_+ - u)(u_- - u).$$

The sign of the second term in Eq. (5.10) is to be chosen to agree with that of \dot{u} . With $a = 0$ this reduces to $d\phi/du = \pm l[B(u)]^{-\frac{1}{2}}$, whose solution in terms of Jacobi functions is immediate. The general case requires elliptic integrals of the third kind, which are clumsier to deal with and not very illuminating; for this reason we avoided detailed discussions of exact solutions in the previous sections. For purposes of illustration, however, we think it is instructive and not too painful to work out one example in detail, and we accordingly derive here an exact formula for the deflection of a beam of light confined to the equatorial plane in the Kerr field.

The total deflection $\Delta\phi$ is obtained from Eq. (5.10) on integrating the right-hand side over a contour extending from $u = 0$ to the branch point $u = 1/d$ at pericenter and back to $u = 0$ again. The first term, being analytic, does not contribute

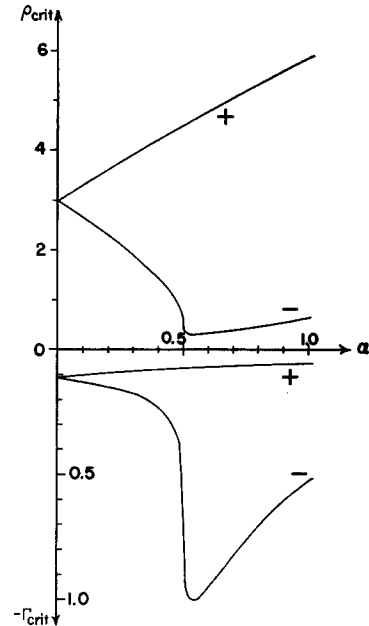


FIG. 11. Values of critical radii and corresponding critical energies, calculated from Eq. (5.8) for $0 \leq \alpha \leq 1$. Curves labeled (+) have $\lambda > 0$; those labeled (-) have $\lambda < 0$. ρ_{crit} gives the minimum radius—in units of $2m$ —for which stable bound orbits are possible (excluding those orbits which penetrate the inner horizon and bounce back onto another sheet of the manifold).

to the total path integral, so one is left with

$$\Delta\varphi = 2 \int_0^{1/d} \frac{A(u)}{D(u)} \frac{du}{[B(u)]^{1/2}}. \quad (5.11)$$

To bring this to standard form, split the rational portion of the integrand into partial fractions, as

$$\frac{A(u)}{D(u)} = \frac{A_+}{u_+ - u} + \frac{A_-}{u_- - u},$$

and write the cubic $B(u)$ as

$$\beta(l + a)^2(s_1 - u)(s_2 - u)(u - s_3)$$

with $s_1 \geq s_2 \geq 0 \geq s_3$. By definition, $s_2 = 1/d$; the remaining two zeros can be expressed in terms of l , a and d as follows:

$$s_1 = (Q + P - \beta)/2\beta d, \quad s_3 = -(Q - P + \beta)/2\beta d, \quad (5.12)$$

where

$$P = d(l - a)/(l + a), \quad Q^2 = (P - 2\beta)(P + 3\beta)$$

have been chosen to agree as closely as possible with Darwin's notation.

Introducing the further parameters

$$k^2 = \frac{s_2 - s_3}{s_1 - s_3}, \quad \alpha_\pm^2 = \frac{s_2 - s_3}{u_\pm - s_3}, \quad \sin^2 \psi_0 = \frac{-s_3}{s_2 - s_3}$$

one obtains after some manipulation

$$\begin{aligned} \Delta\varphi &= 4(l + a)^{-1}(d/Q)^{1/2} \{ A_+(u_+ - s_3)^{-1} \\ &\quad \times [\Pi(\alpha_+^2, k) - \Pi(\psi_0, \alpha_+^2, k)] + A_-(u_- - s_3)^{-1} \\ &\quad \times [\Pi(\alpha_-^2, k) - \Pi(\psi_0, \alpha_-^2, k)] \}, \end{aligned} \quad (5.13)$$

where $\Pi(\alpha^2, k)$, $\Pi(\psi_0, \alpha^2, k)$ are, respectively, the complete and incomplete elliptic integrals of the third kind. It can be shown that the above result reduces to $\Delta\varphi = \pi$ when $\beta = 0$. This is of course to be expected, since the Kerr metric becomes flat for $\beta = 0$, and serves as a check on the intermediate calculations. In the limit $a \rightarrow 0$ one finds $A_+ = 0$, $A_-/(u_- - s_3) = l$, and $\alpha_- = 0$, so

$$\begin{aligned} \Delta\varphi &\xrightarrow{a \rightarrow 0} 4(P/Q)^{1/2} [K(k) - F(\psi_0, k)] \\ &= 4(P/Q)^{1/2} F(\psi_1, k), \end{aligned} \quad (5.14)$$

with $\cot \psi_1 = (1 - k^2)^{1/2} \tan \psi_0$, in agreement with Darwin's result.

From Eq. (5.13) one readily deduces the corrections to the familiar deflection formula due to rotation of the central body. We assume β/d and a/d small, and keep terms to order $\beta a/d^2$. Setting

$$\Delta\varphi = \pi + \delta,$$

where δ is the deflection angle as usually defined, we find

$$\delta \approx \frac{2\beta}{d} + \frac{2\beta a}{d^2} = \frac{4m}{d} \left(1 + \frac{a}{d} \right). \quad (5.15)$$

This result has also been obtained by Skrotskii³⁰ using the weak-field metric of Landau-Lifshitz, and from a more general viewpoint by Plebański.³¹ The value for the correction term a/d is difficult to estimate in the case of the sun, since its angular momentum is not well known. Assuming essentially uniform rotation throughout its interior, at the rate $14.3^\circ/\text{day}$ observed for sun spots near the equator, one computes $a \simeq 1.9 \text{ km}$ and consequently $a/d \simeq 3 \times 10^{-6}$ for a light ray grazing the sun's disk, which is undetectable by several orders of magnitude. Measurements of the solar oblateness are not inconsistent with a value of a/d several times as large as this³²; however, this would require a mass quadrupole moment Q_\odot of order $10^{-4} M_\odot R_\odot^2$, which in turn would contribute a correction term to δ of about the same magnitude.³³

Note added in proof: It has been pointed out by C. V. Vishveshwara (University of Maryland Tech. Rept. No. 589) that if one considers "stationary" sources and observers (i.e., those whose world lines are the Killing trajectories $\partial/\partial t$), then the surface of infinite red shift occurs at $g_{tt} = 0$, which does not coincide with the null horizon in the Kerr case (unless $a = 0$).

ACKNOWLEDGMENTS

We are much indebted to Professor A. Schild and members of the Center for Relativity Theory of the University of Texas for their hospitality and many stimulating conversations. We are also grateful to Brandon Carter for many helpful discussions, and for placing several unpublished results at our disposal.

Added in proof: I acknowledge above all my debt to a dear friend, collaborator and co-author, whose penetrating insight and ingenuity were responsible for bringing this work to a successful conclusion. To the extent that this paper conveys these traits, it bears the imprint of his thought, and stands here as a memorial to his accomplishment.—R.W.L.

³⁰ G. V. Skrotskii, Dokl. Akad. Nauk SSR 114, 73 (1957) [English transl.: Soviet Phys.—Doklady 2, 226 (1957)].

³¹ J. Plebański, Phys. Rev. 118, 1396 (1960).

³² R. H. Dicke, Nature 202, 432 (1964), has suggested that the interior of the sun might have a rotational period as small as 25 h, without leading to an unreasonably large visual oblateness or violating stellar structure theory. This would increase a/d to 6×10^{-5} , still too small to be significant.

³³ The quadrupole field adds to Eq. (5.15) a term $\frac{1}{2} (4m/d) (k/d)^2$, where $Q = mk^2$ is the quadrupole moment. Taking a gravitational oblateness of 5×10^{-6} for the sun, as suggested by Dicke,³² we calculate $(k/d)_\odot = 7 \times 10^{-5}$.